2024
https://fupress.org/journal

Research on the Application of Visual Design Based on Artificial Intelligence in Internet Medical Platform

Elena Müller

PhD Candidate, Department of Computer Science and Media Technology, Linnaeus University, Växjö, Sweden
* **Corresponding Author:** elena.novak.ai.design@lnu.se

ARTICLE INFO

Received: 10 Feb 2024
Accepted: 27 Apr 2024

ABSTRACT

Medical devices may connect to the Internet and interact with one another through the Internet of medical things (IoMT) platform, allowing for effective monitoring and diagnosis in the healthcare industry. Medical images such as computed tomography (CT) scans are crucial components of the IoMT platform and may be used to study infectious diseases as part of the patient's clinical record. Doctors have to assess the 3D shape of a tumor depending on their expertise with CT imaging, which is a time-consuming and complex process since CT imaging can only offer 2D information about organs. Hence, in this paper, we proposed a three-dimensional visual design of 2D lung CT images and automatic classification of lung cancer using Artificial Intelligence on an internet medical platform. Initially, we obtained 2D lung CT images from the IoMT platform and preprocessed them using a Laplacian filter. Then the segmentation of the tumor region from CT images is performed using Otsu's N Thresholding technique. The 3D visual design of the segmented tumor is reconstructed using Bio Volume-Deep Convolutional Neural Network (BV-DCNN) to enhance the visual quality and analyze the hidden information. The significant features for lung tumor classification were extracted from a 3D visual model using Grey Level Co-occurrence Matrix (GLCM) method. Finally, the lung tumor images were classified either into benign or malignant categories using Multi-Scale Long Short Term Memory (MLSTM). The results showed that the proposed classification method is superior to the existing methods in lung cancer classification.

Keywords: Internet Medical Platform, Visual Design, Computed Tomography (CT), BioVolume – Deep Convolutional Neural Network (BVDCNN), Multiscale Long Short Term Memory (MLSTM).

INTRODUCTION

The numeral of 'intelligent Medical Internet of Things' (IoMT) devices distributed online have been steadily expanding, achieving 21.45 billion in 2018 and predicted to hit 76.45 billion in the next decade. The application of IoMT in the health business accounts for a substantial share of them. Cyber attacks against IoMT, on the other hand, are not new, and they can have disastrous repercussions. The majority of IoMT devices are defenseless. Cyber attacks are becoming more sophisticated as IoMT devices become more widely used, posing a bigger danger to the efficient functioning of not only connected systems and also the entire internet (Zhang et al., 2020).

IoMT and Artificial Intelligence (AI) are two connected disciplines of technology that have an impact on the design and enhancement of suitable individualized healthcare systems. IoMT-based healthcare systems can benefit from AI in a variety of ways. IoMT technologies enable a reduction in the worldwide cost of preventing chronic illnesses. The outcome of such platform medical data analytics improve the relevance of data interpretations and reduce the time it takes to assess data outputs. In addition, modified preventive strength coach, a new system, has been established. It keeps track of memories and can be used to interpret and comprehend data on health and well-being (Bhoi, Mallick, Liu, & Balas, 2021). **Figure 1** represents the impact of IoMT in medical health care.

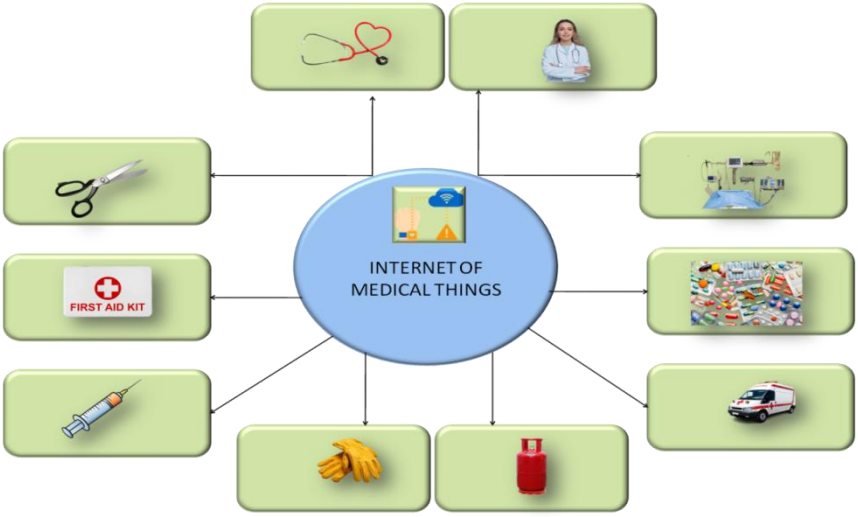

Figure 1. Impact of IoMT in Medical Health Care

In practically every aspect of life, particularly science and medicine, AI is used to uncover various technical advances to tackle complicated problems. AI is a field of computer science that focuses on a machine's ability to mimic and even improve intelligence. Dealing with comprehensive research investigations meant at behind immediate executive and create answers to difficult challenges from side to side education and data-heavy computerized and simulation analyses is one of the predicted responsibilities in life and therapeutic science. A person's lifestyles, health records, experienced encounters with organizations, laboratories, imaging studies, diagnoses, prescription drugs, conducted surgical techniques, and consulted providers are all included in healthcare data (Ahmed, Mohamed, Zeeshan, & Dong, 2020).

AI can exceed conventional physicians in several areas, according to health personnel, especially practitioners. The wider populace has less content knowledge than AI experts and medical professionals, but they are the last user of health check AI. The public's acuity of AI in healthiness heed is critical. Public perceptions and attitudes regarding AI in therapeutic mind could confuse AI product development, such as collecting enough information from the communal for apparatus research at an early stage. In the middle and late stages, however, municipal receiving of AI products may have an impact. They believe that the success of the medical AI business is in part determined by whether practitioners in adjacent professions have a thorough sympathetic of the individuals perceptions of AI in medical care (Gao, He, Chen, Li, & Lai, 2020).

In past years, Internet hospitals have sprung up throughout China. AI is now a rising issue in the medical area. Decision and therapies can benefit from AI's ability to propose improved drug alternative and perform specific procedures. It's possible to prevent food-borne illnesses by training an AI system using Twitter data, according to health researchers now at Casino State health Department. More clinical diagnosis detection and management can be achieved through the use of more complete medicine data. Deep Mind researchers lately built a model that may detect acute kidney damage 48 hours ahead of time using a deep learning approach (X. Jiang et al., 2021). In this paper, research on the application of visual design based on artificial intelligence in internet medical platforms is studied.

The further part of the paper is divided into four parts, literature review and problem statement, proposed methodology, result and discussion, and conclusion.

RELATED WORKS

These numerous odontogenic keratocystic lesions are found in many of the conditions in the study by Eryong and Li (2021). There were many odontogenic keratocysts on a 12-year-old female adolescent from our clinic. There were no other abnormalities that could be linked to a medical condition. The use of fine-grained data in the study by Garg (2020) customized medicine allows for the identification of precise deviations from normal. Engineers used 'Digital Twins' to study these new data-driven health care systems, both philosophically and ethically. Artifacts were linked together utilizing digital approaches that constantly show how they're doing. Data

formats and explanations imposed on the data can be used to identify disparities in mortality. Examined are Digital Twins' ethical and societal implications. Health care is becoming more and more data-driven. Providing effective measures for social equality, this move toward has the possible to be a communal 'equalizer'.

An allergic rhinitis outbreak would be a worldwide problem (Ahmed & Ali, 2020). In Taiwanese institutions, the most common treatment therapies are China drugs. Allergy rhinitis affected established Chinese tablets solutions for lung illnesses. When it comes to the treatment of allergies in Taiwan, they compared traditional Chinese medicine with conventional medicine. Radiation is avoided, outpatient therapy is possible, and diagnosis times are reduced with the use of high-dose-rate brachytherapy (Shahabaz & Afzal, 2021). Increasing dose dispersion with a single-stepping emitter could be accomplished by altering the latency at each dwell point. HDR "brachytherapy" treatments must be carried out correctly because the shorter processing times necessitate no error-checking and inaccuracies could cause harm to patients. To ameliorate rural areas, Bo and Wen (2022) proposed a sewage treatment system and associated equipment. "Physicochemical' and "organochlorine" pesticide residues have been found in earth sample from vegetables fields in "Zamfara" Stat, A "GC-MS" was used to examine the results of the testing method.

The factors that lead to stroke can be identified in an investigation. For big data, a correlation of relevant factors was shown using the MIoT platform (C. Guo et al., 2020). In research, the authors present a unique non-natural intelligence-basis semantic IoT mix tune design for always IoT devices and supporting top quality services. Garbuio and Lin (2019) examined AI-driven medicine care businesses and highlights emergent commerce replica paradigms that business people from across the world are employing to transport AI products to clients. Aman et al., (2021) focused on the IoMT architecture, implementations, capabilities, and privacy advancements that have been developed in the fight against COVID-19. Sun, X. Jiang, Ren, and Y. Guo (2020) gave a detailed evaluation of how to implement the fast processing of data of medical big data, as well as the disposal of increased healthcare care. The benefits of cloud technology, advanced analytics, and artificially intelligent technologies to the IoMT are also discussed.

The study discusses how edge-IoMT-based solutions can be used in medicine to reduce the workload of healthcare professionals and providers while also allowing patients to live independently during the COVID-19 outbreak and providing high-quality treatment. The study provides an unfathomable education explanation for fitness information that intelligently predicts which meal is supposed to be supplied to which unwearied based on bug and added factor like heaviness, fat, proteins, and fibers (Iwendi, Khan, Anajemba, Bashir, & Noor, 2020). The major goal of Manimurugan et al. (2022) is to use medical data and medical imagery to classify data and forecast cardiac disease. The suggested model is a two-stage categorization and prediction method for medical data. The study begins with an overview of IoMTs before moving on to a structure for IoMT. It then goes on to describe the production systems of the health service and how they are mapped into the design and architecture.

Problem Statement

In several countries, Co-opting the IoMT with some other strategies has been successful in combating COVID-19, enhancing front-line worker safety, enhancing productivity, and lowering mortality rates. Significant advancements in terms of file and technique, as well as security, have been made, which have been amplified by the quick and AI associated with the usage of IoMT around the world. Several ongoing studies suggest that integrating security measures with technology can lead to the uptake of secure IoMT applications. Furthermore, when new IoMT techniques merge into Artificial Intelligence more feasible solutions become available. The healthcare industry is being transformed by artificial intelligence. Process automation, drug development, diagnostics, mining medical data, reporting patient experience, and maintaining more are all possible uses. Most crucially, AI has various applications in analyzing vast amounts of unstructured data and is providing clinicians with accurate insights into any patient's health, resulting in better and more individualized care delivery outcomes.

METHODOLOGY

The primary aim of this paper is the application of visual design based on artificial intelligence in internet medical platforms is studied. **Figure 2** depicts the proposed methodology.

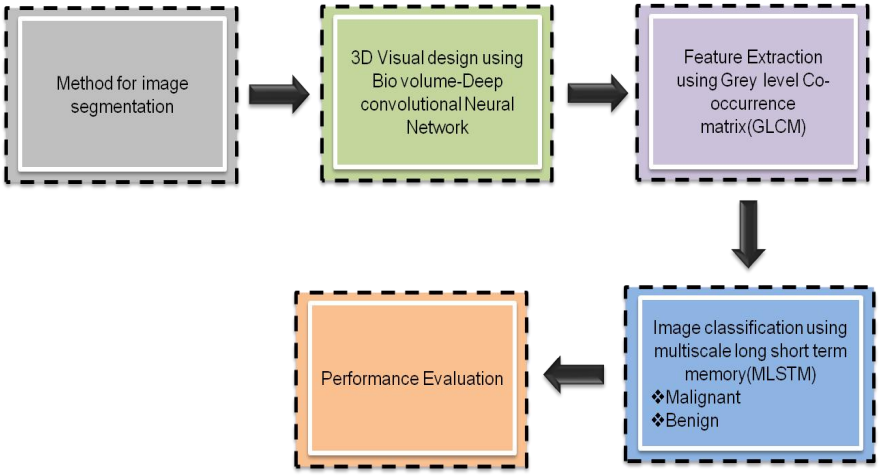

Figure 2. Proposed Methodology

Dataset

In partnership with "Sun Yat-sen University Cancer Center" "(SUCC)", a position enter "Laboratory of Oncology" in Southern part of China, we developed a massive dataset. This dataset contains 965 "digitalized" histology WSIs obtained from 859 lung cancer patients and 85 healthy people, and it contain classes of lung cancer (Wang et al., 2019).

Image Preprocessing Using a Laplacian Filter

The goal of lung ultrasound image preprocessing is to increase representation superiority. It employs histogram equalization to improve the effort imagery normal. It should be noted that for classification, 80 percent of the data was chosen at random. The remaining 20% was allocated to testing. The training set of data should be much larger to get more accurate findings. The unprocessed CT scan picture is preprocessed to improve segmentation and raise the system correctness in the after that stage of thresholding. This approach also penetrates and separates an object where the edge boosting property of the Laplacian filter produces noticeable changes in the grey levels of boundary points. As can be seen by using the laplacian, any filters method must be adjusted in order to take use of the classifier's edge enhancement. Laplacian filter consists of a series of steps that increase image quality. It is accomplished by continuously reorganizing the image's Gray level pixels within the software algorithms by decreasing the image's Gray level pixels. This process might have unfavorable effects when applied to low-color pictures (such as the gradient visible in the image). Color depth (the number of specific grey colors) in an 8-bit image with a grey level 9 small piece palette, for example, is further lowered. The Laplacian filter is best done when practical to photos with a substantially larger color strength than pallet size, such as continuous data or 16-bit grey images. It also removes the noise from the background. **Figure 3** show the preprocessing "output" of the image.

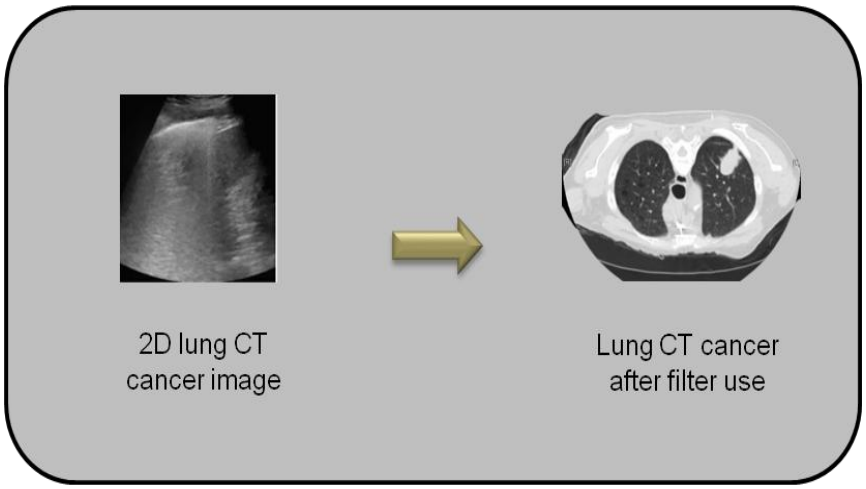

Figure 3. Preprocessing Output of the Image

Otsu's N ROI Thresholding Method for Image Segmentation

The segmentation of the tumor region from CT images is performed using Otsu's N ROI thresholding technique. As long as the image has a heterogeneous histogram, the globally filter method can recover the target object from the surrounding noise. In this case, a limit will not eradicate the entire reference image since the image pixels of lungs are so similar. To erase the backdrop from an image, a process is necessary. The threshold image that results contains both nonbody and body areas. The image's white portion depicts non-body voxels, whereas the black part depicts body voxels. The non-body area contains the lobes of the lungs. We used a 2D connected component approach to remove the background. The non-body component is eliminated from the lungs' sides and the voxels principles are set to backdrop standards in the background removal technique.

3D visual design using Bio Volume – Deep Convolutional Neural Network (BV DCNN)

The 3D visual design of the segmented tumor is reconstructed using BV-DCNN to enhance the visual quality and analyze the hidden information. A more acceptable approach would be to give these indicated regions a higher weight because they have a higher likelihood of becoming cancer. In other words, as the CNN misclassify annotate place, a harsher penalty is applied, guiding the CNN to acquire more valuable and "discriminative patterns". We teach a scrap base CNN by reducing the biased 'cross-entropy' failure purpose as follows:

$$\mathcal{L} = \sum_{d\in U}\sum_{\mathscr{p}=1}^{G} -\alpha H_{\mathscr{p}} \log I(s=\mathscr{p}|d;F,j) + \sum_{d\notin U}\sum_{\mathscr{p}=1}^{G} - H_{\mathscr{p}} \log\ I(s=\mathscr{p}|d;F,j) + \lambda\|F\|_2^2 \quad (1)$$

where $\theta = \{F, j\}$ stands for the BVDCNN model's parameters, $I(s=\mathscr{p}|d)$ for the productivity likelihood for the $\mathscr{p}$ the division given the key in sub-window in which $s\epsilon\{1, 2, \ldots . G\}$ and $H_{\mathscr{p}}$ for the BVDCNN-level label. The sum figure of lessons is G.

The uncouth footnote facade put is denoted by U. The equilibrium heaviness flanked by the annotate and nonannotated area classifiers is α. In this article, the $\alpha \epsilon [1,5]$ range of α values was explored, with being set to 2 using grid search. Furthermore, γ manages the transaction among statistics defeat and 'regularization'.

However, because CNN intensively slide in excess of the BVD and patch split overlapping regions with its nearer, this technique invariably lead to mark being without a job during presumption. In BVDCNN, however, there are outliers or mimics with high probability because of the variability of histological features. They frequently harm the quality of future BVDCNN holistic feature representation, lowering picture organization presentation. To address the aforesaid challenge, we use rich contextual knowledge to help us choose better features. A tumor area is typically larger than a patch, resulting in far above the ground probability scores showing in an intense region. To put it another way, the average chance of a tumor region is high. On the other hand, even if a "high probability" outlier occurs in a typical hankie chunk, it is easily drinkable out owing to the chunk low standard likelihood. We expressly refer to a block as,

$$\begin{bmatrix} R_{1,1} & R_{1,2} & \cdots & R_{1,q} \\ R_{2,1} & R_{2,2} & \cdots & R_{2,q} \\ \vdots & \vdots & \vdots & \vdots \\ R_{q,1} & R_{q,2} & \ldots & R_{q,q} \end{bmatrix} \quad (2)$$

Where q denotes the numeral of overlap patches in every line (column) and $R_{R,L}$ denotes the patch in block A's Rth row and Lth column, where $R, L \epsilon\{1, 2, \ldots . A\}$. $I_{r,l} = (I^1{}_{r,l}, I^2{}_{r,l}, \ldots, I^G{}_{r,l})$

To calculate the average probability inside a block for each class, this is then used to determine whether the discriminative block surpasses a certain threshold. **Figure 4** represents the conversion of 2D images to 3D images.

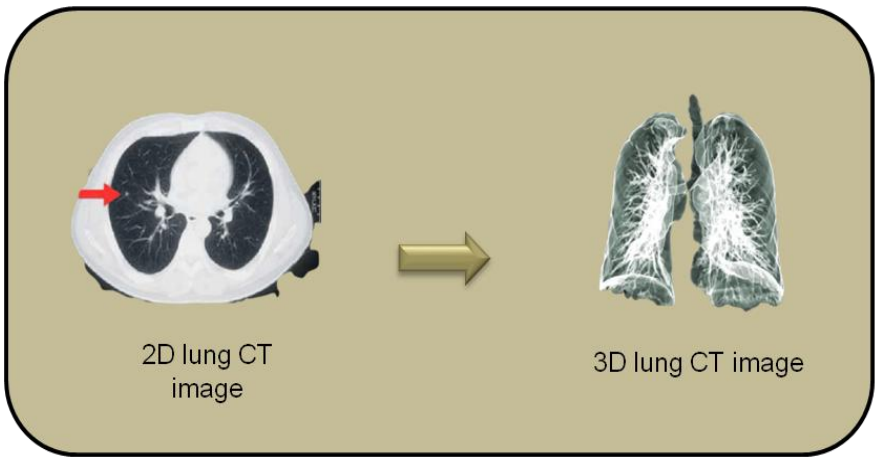

Figure 4. Conversion of a 2D Image to a 3D Image

It is standard procedure to use bricks as outputs to the training BVDCNN, and the produced probabilities mappings are then summed so that the mean possible values may be calculated.

Feature Extraction Using Grey Level Co-Occurrence Matrix (GLCM)

The significant features for lung tumor classification were extracted from a 3D visual model using the GLCM method. It is a quantifiable surface investigation practice that analyzes the spatial dependence matrix in Gray levels by considering the 'spatial' association of GLCM "pixels". The GLCM represent the pixel decision in a set spatial background, giving it unique properties. After this approach, the experiential size is eliminating as of the medium. The corresponding pixel size is shown in the $(j_1, j_2|t_1,$ and $t_2)$ matrix t_1, t_2 respectively. Higher-order statistical texture details are extracted using the GLCM approach. An early re-quantization to collect the network typically reduces the image in the full Gray dimensions. The GLCM is written as equation (3)

$$A(\theta) = \left(\frac{b(z,x)}{\theta}\right), 0 \le z \le C_b, 0 \le x \le Qmax \tag{3}$$

Where C_b denotes average Gray level quantities Qmax denotes greater duration, and z, x denotes matrix value sizes. The Gray level value of each $b(z, x)$, and x is represented by z.

Using pre-trained networks without investing time and effort in training is possible using feature extraction. A pre-trained network was utilized to extract learned features, which were then used to train a classifier. Information that has been enhanced in integrity for the purpose of better use, analysis, and presentation in healthcare settings Conventional medical IoMT technologies comprises collecting data and giving a predetermined conclusion to the end-users of the system. Machines must be educated with a range of input data in order to give valuable insights and predictions from IoMT. IoMT will practitioners in healing their customers because they don't have the time or resources to deal with all of this information. In ultrasound image collections, computerized feature extraction testing is carried to remove unnecessary features. It takes less data to use the feature selection method. Models for extracting features from program data are commonly used.

Image Classification Using Multiscale Long Short Term Memory (MLSTM)

Finally, the lung tumor images were classified either into benign or malignant categories using the MLSTM method. Equations (4) and (5) show the prescription for both chamber structures in the CNN network given a string of ethics $v^{(1)}$, $v^{(2)}, v^{(3)}, \ldots\ldots. v^{(s)}$ as input data:

$$a^s = \tan a\left(wh^{(s-1)} + Zv^{(s)} + e_g\right)' \tag{4}$$

$$I^{(s)} = ja^{(s)} + e_{Y'} \tag{5}$$

Wherever the heaviness matrix that point to the association between two images are w, Z, and j. w links the before concealed lump to the at present veiled nodule, Z links the effort swelling to the concealed bump, and j links the concealed swelling to the production lump. The bias vectors are $e_{Y'}$ and e_g. At any given moment, s represents the input value, a concealed value, and $I^{(s)}$ the output value. A nonlinear activation function is tan a. In equation (4), the initialization value of a is zero. According to equation (4), the manufacture is together firm by the input $v^{(s)}$ at times, and the $a^{(0)}$ will approach infinity or zero as time passes. In the backpropagation phase, this will reason the incline to vanish or blow up. In extra language, when significant in sequence is located far away starting the present site, CNN will not be able to properly use it. CNN is unable to address the issue of long-term

dependency. To tackle this problem, the MLSTM network is proposed. The MLSTM uses a gating mechanism to remember past knowledge while simultaneously filtering out irrelevant data. In CNN, the MLSTM is effective at solving the lengthy dependency problem.

Input gate

$$r^{(s)}=\sigma\left(Y_r v^{(s)} + Z_r a^{(s-1)} + e_q\right)' \tag{6}$$

Output gate

$$i^{(s)} = \sigma\left(Y_i v^{(s)} + Z_0 a^{(s-1)} + e_i\right), \tag{7}$$

Candidate cell value

$$\tilde{i}^{(s)} = \tan h\left(Y_k v^{(s)} + Z_k a^{(s-1)} + e_k\right) \tag{8}$$

Cell state

$$c^{(s)} = r^{(s)} * \tilde{k}^{(s-1)} + q^{(s)} * k^{(s-1)} \tag{9}$$

MLSTM output

$$a^{(s)} = i^{(s)} * \tan a\left(k^{(s)}\right) \tag{10}$$

The logistic sigmoid function is denoted by σ, and the Hadamard product operation is denoted by $*$. Weight matrices include Y_r, Y_i, Y_k, Z_r, Z_0, and Z_k. Bias vectors are the vectors e_q, e_i, and e_k.

The grouping system equation is as follows,

$$\begin{aligned} z^{(1)} &= \left[V_{1,}\, V_{1+w}, \ldots V_{1+w(q-1)}\right] \\ z^{(2)} &= \left[V_{2,} V_{2+w}, \ldots V_{2+w(q-1)}\right] \\ z^{(a)} &= \left[V_{a,} V_{a+w}, \ldots V_{a+w(q-1)}\right] \\ z^{(w)} &= \left[V_{w,}\, V_{2w}, \ldots V_{wq}\right] \end{aligned} \tag{11}$$

Where $z^{(a)}$ is the ath group. w denotes the number of groups, $z^{(w)} = \left[V_{w,} V_{2w}, \ldots V_{,w,\,q}\right]$ where denotes the spectral vector.

The spectral distance between distinct groups will be reduced with this technique, and the majority of the spectral range will be covered.

We adopted the supplementary thrashing role; the absolute loss purpose is shown in equation (12)

$$N^{joint} = -\frac{1}{q}\sum_{a=1}^{q}\left[b_a \log\left(\hat{b}^{joint}{}_a\right) + (1-b_a)\log\left(1-\hat{b}^{joint}{}_a\right)\right], \tag{12}$$

$$N^{Bi-LSTM} = -\frac{1}{q}\sum_{a=1}^{q}\left[b_a \log\left(\hat{b}^{Bi-LSTM}{}_a\right) + (1-b_a)\log\left(1-\hat{b}^{Bi-LSTM}{}_a\right)\right] \tag{13}$$

$$N^{CNN} = -\frac{1}{q}\sum_{a=1}^{q}\left[b_a \log\left(\hat{b}^{CNN}{}_a\right) + (1-b_a)\log\left(1-\hat{b}^{CNN}{}_a\right)\right] \tag{14}$$

$$N = N^{joint} + N^{Bi-LSTM} + N^{CNN}, \tag{15}$$

Where N stands for the loss function and b_a and b_a stand for the ath training sample's predicted and real labels, respectively. The superscripts joint, MLSTM, and CNN, respectively, refer to the entire framework, the MLSTM network, and the 3-D CNN. The number of the training sample is represented by the variable b_a.

Algorithm 1 depicts the suggested MLSTM method's implementation technique.

Algorithm 1: MLSTM procedure

Input

1. HSI labeled as such

2. The patch's size, and the number of primary components retained P ω.

Step 1

To feed the MLSTM circuit, partition the spectroscopic cube into w phases to every point in the HIS using Equation (9).

Step 2

In order to feed the 3-D CNN, remove a patch of the same width as the lowered HIS from the vicinity from each pixel

Step 3

If want to start with data that has a bell curve, then use random numbers with an error margin of zero to set up the MLSTM-CNN with an original weight of 0.

Step 4

LSTM and 3-D extract the spectrum characteristics and geometric structure from HIS, respectively. Integrate development of soft skills into the MLSTM-CNN. Once the retrieved features have been categorized, Linear function is used to do so MLSTM-CNN settings are fine-tuned using back propagation algorithm after the smaller version MLSTM method is used to maximize performance.

Step5

Step 1 and Step 2 information should be entered into MLSTM-CNN for each pixel inside the HSI to forecast a HIS values.

Output

Outcomes one per byte in HIS.

Benign

The term "benign tumor" refers to an abnormal clump of cells that is not cancerous. Cells can form anywhere on or in the body if they multiply excessively but do not die properly. A cancerous lump is not malignant. More slowly spreading, with clearer boundaries, and not affecting any other parts of your body.

Malignant

A cancerous growth is a cancerous growth. They go through the body's circulatory and lymphatic systems. Cancer is the term for this process. Anywhere in the body can be affected by metastasis, but it is more common in the hepatic, organs, heart, and osteoporosis than in any other organ. These maximum feature pictures effectively determine the malignancy parts of the lung in the diagnostic imaging, which aids the scanner computer's computer efficiency of the algorithm.

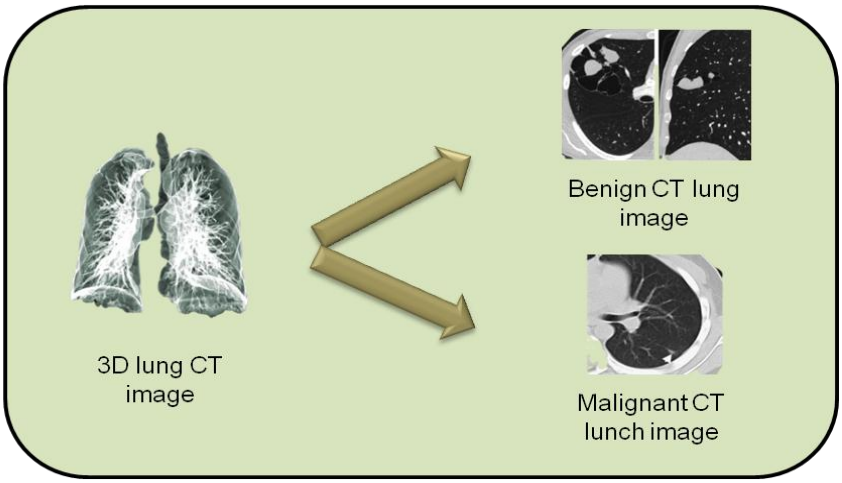

Figure 5. Output of Proposed Method

The cancer risk of the observed tumors was then determined by comparing them to the identification tumor. In order to arrive at a final assessment of malignancy, the three models' outputs were pooled.

RESULTS AND DISCUSSION

The proposed method is contrasted with existing methods such as “K-Nearest Neighbors method” (KNN (Kadry et al., 2020)), the “Support Vector machine method” (SVM (Khan et al., 2019)), the “Naïve Bayes method”

(NB (Manickavasagam & Selvan, 2019)), and “Long Short Term Memory method” (LSTM (Ter-Sarkisov, 2022)). Accuracy and threshold, success rate, sensitivity, accuracy, specificity, and precision were taken as study parameters for this study.

The classification accuracy and threshold level of the proposed method are shown in the following graph. **Figure 6** shows a plan of the test accuracy that shows the effect of the threshold level on overall classification accuracy.

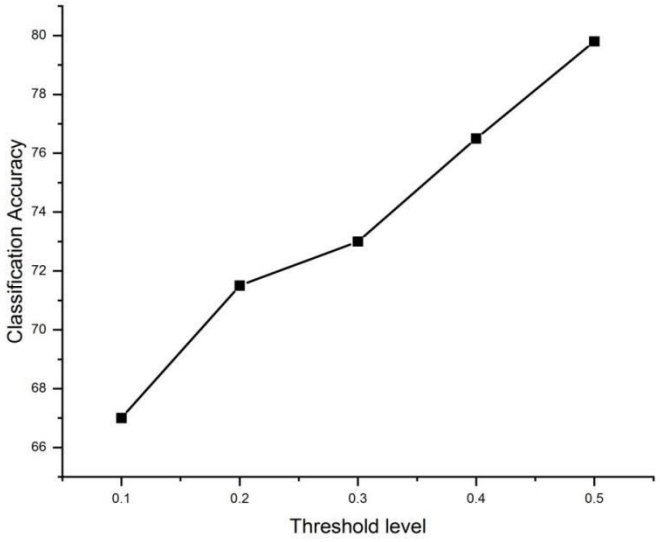

Figure 6. Plot of the Test Accuracy that Shows the Effect of the Threshold Level on Overall Classification Accuracy

The graph shows the significance of the suggested method in terms of overall accuracy and threshold level. The graph depicts that increasing the threshold values beyond 0.43 does result in a significant increase in inaccuracy.

Success rate

The success rate is the fraction or percentage of attempts to complete a method or task that are successful. It could refer to the success rate of call establishment. The success rate is defined as it is the ratio between the come to of thriving runs plus the total body of run. **Figure 7** shows a comparison of the success rate for proposed and existing methods.

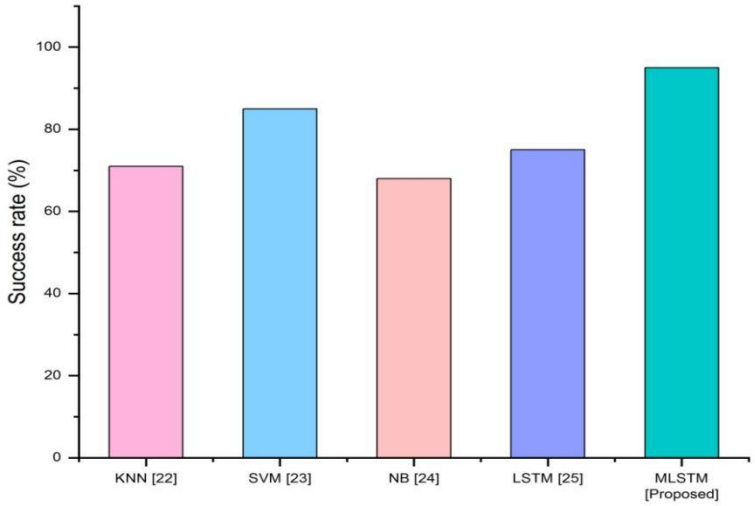

Figure 7. Contrast of Success Rate for Suggested and Existing Methods

When the suggested method is compared with the existing method interns of its success rate, the proposed method shows more significance than the other methods. The existing method shows drawbacks like their efficiency is shorter.

Sensitivity

The sensitivity of that algorithm is derived by dividing the number of correctly identified tests. **Figure 8** shows the comparison of sensitivity for proposed and existing methods.

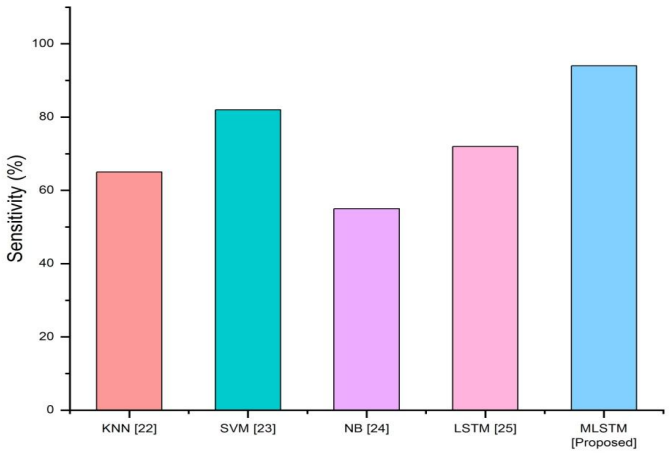

Figure 8. Comparison of Sensitivity for Proposed and Existing Methods

The sensitivity of the proposed method shows more significance than the proposed method. The drawback of the traditional method includes different random weight initialization.

Accuracy

The accuracy is defined as it is the ratio between the number of correctly classified sample polarity and the number of marked samples polarity.

$$\text{acc} = (\text{sens})(\text{prev}) + (\text{spec})(1 - \text{prev}) \tag{16}$$

Where ‘acc’ is accuracy, ‘sens’ is sensitivity, ‘prev' is prevalence, and 'spec' is specificity. **Figure 9** depicts the

comparison of the accuracy of proposed and existing methods.

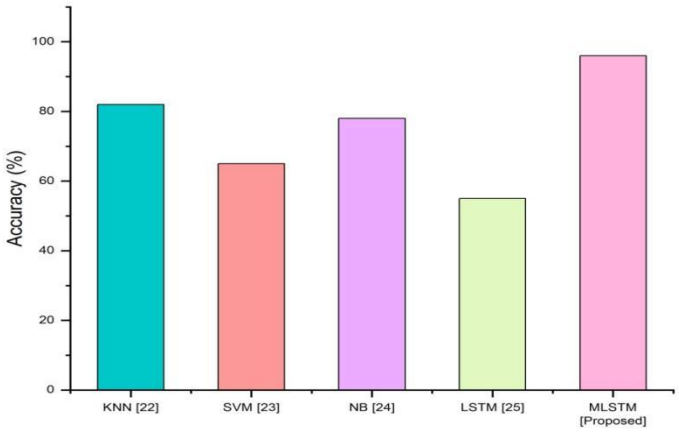

Figure 9. Comparison of Accuracy of Proposed and Existing Methods

The proposed method shows more significance than the existing methods interns of accuracy. The existing methods show zero probability problems.

Specificity

Specificity can be defined as the quality or state of being specific. It is the ratio of the product of several true negatives and the number of true negatives.

$$\text{spec} = (\text{number of true negatives}).(\text{number of true negatives} + \text{number of false positives}) = (\text{number of true negatives}).(\text{total number of samples}) \quad (17)$$

Where 'spec' is specificity. **Figure 10** depicts the comparison of the specificity of proposed and existing methods.

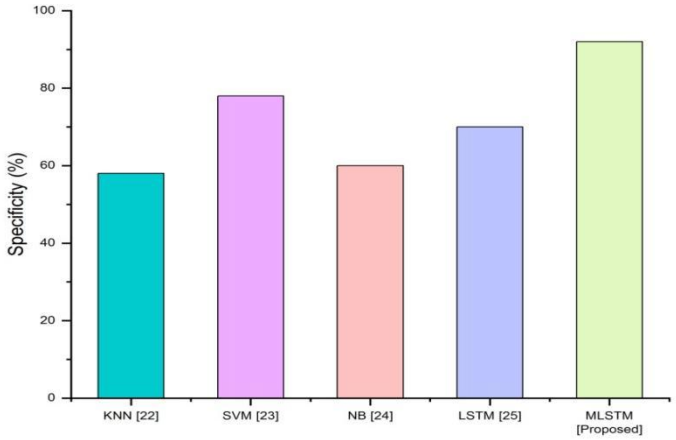

Figure 10. Comparison of Specificity of a Proposed and Existing Method

The proposed method shows more significance than the existing method. The other methods need more memory.

Precision

Precision is also known as positive predictive value. The number of positive class predictions that are positive class predictions is known as precision. It's the ratio of actual positive results to expected positive results. Use the following formula to calculate precision:

$$P = \frac{tp}{tp+fp} \quad (18)$$

Where P is precision, tp is truly positive, fp is false positive. **Figure 11** shows the comparison of precision for proposed and existing methods.

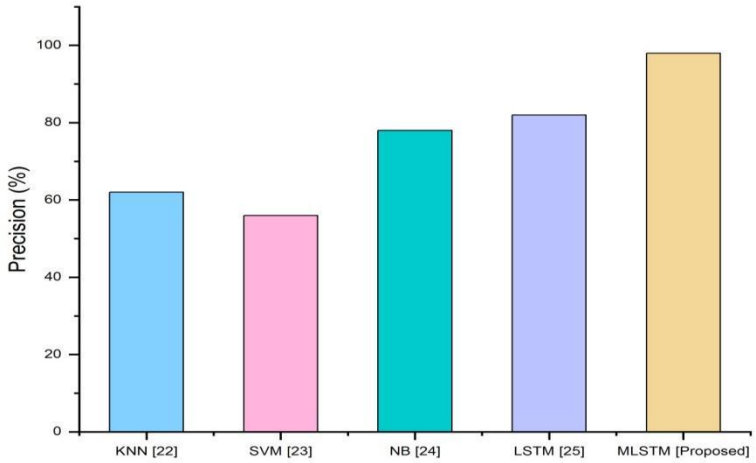

Figure 11. Comparison of Precision for Proposed and Existing Methods

The proposed method shows more significance than the existing method. The traditional methods shows drawback such as, they are significantly slow as the size of data grows and they cannot train for a longer time.

Discussion

In this paper, we proposed a three-dimensional visual design of 2D lung CT images and automatic classification of lung cancer using Artificial Intelligence on internet medical platforms. Initially, we obtained 2D lung CT images from the IoMT platform and preprocessed them using a Laplacian filter. Then the segmentation of the tumor region from CT images is performed using Otsu's N thresholding technique. The 3D visual design of the segmented tumor is reconstructed using BV-DCNN to enhance the visual quality and analyze the hidden information. The significant features for lung tumor classification were extracted from a 3D visual model using the GLCM method. Finally, the lung tumor images were classified either into benign or malignant categories using MLSTM. The results showed that the proposed classification method is superior to the existing methods in lung cancer classification. The KNN method shows the difficulty in choosing the correct picking of the K value. The SVM method is not suitable for the large data set. A small change in the data can cause instability of the NB method. The stop band issues are shown via the LSTM approach. As a result, the new approach is more significant than the old ones. Classifying activity based on relevant predictive indicators is a crucial first step in properly addressing the problem. Traditional AI models can be used for easy prediction tasks, while more complex models are needed for more difficult assignments. The next step is to figure out how to implement the model. Conventional models are useful for determining the feasibility of breaking down large jobs into smaller ones, or whether pre-processing data is required prior to running a job. It takes a long time to create and maintain these rules, but they are quite useful. The accessibility of learning algorithm is another crucial feature of intelligent automation. It's possible for simple models to work with a small amount of data and variables, but advanced models need a big amount of data and multiple examples and situations to get rid of the noise and learn to recognize complex statistical patterns.

CONCLUSION

The research on internet hospital departments and diseases is scant despite China's significant development in the variety of internet hospitals. They allow medical professionals alike to track and avoid issues like chronic sickness, as well as to provide high-quality care even in remote regions. The Internet of Medical Things (IoMT) is a network of medical products, software, systems, and services. With the recent explosion of sensor-based tools, like as wearables and hang devices for remote patient, the IoMT stands out from other IoT applications. This is strengthened by the combination of linked medical devices and an abundance of patient data. Its expansion is being fueled by the increasing number of interconnected medical devices that produce, collect, analyze, and send data. Using these gadgets, healthcare providers can communicate with each other and send data to the cloud or

internal systems. IoMT networks necessitate a high level of system security in order to protect patient safety and confidentiality. Tailored and community medicine could be steered more effectively with AI and its implementation in healthcare, thanks to its numerous computational advantages. AI's rise in healthcare is evident, but it will take intelligent frameworks to link reporting and analysis systems in such a way that specialists from other fields can do measurements and predictive analyses to promote better sector patient care.

REFERENCES

Ahmed, B., & Ali, A. (2020). Usage of traditional Chinese medicine, western medicine and integrated Chinese-western medicine for the treatment of allergic rhinitis. *Official Journal of the Zhende Research Group*, *1*(1), 1–9.

Ahmed, Z., Mohamed, K., Zeeshan, S., & Dong, X. (2020). Artificial intelligence with multi-functional machine learning platform development for better healthcare and precision medicine. *Database*, *2020*.

Aman, A. H. M., Hassan, W. H., Sameen, S., Attarbashi, Z. S., Alizadeh, M., & Latiff, L. A. (2021). IoMT amid COVID-19 pandemic: Application, architecture, technology, and security. *Journal of Network and Computer Applications*, *174*, 102886.

Bhoi, A. K., Mallick, P. K., Liu, C. M., & Balas, V. E. (Eds.). (2021). *Bio-inspired neurocomputing* (Vol. 310). Springer.

Bo, Y., & Wen, W. (2022). Treatment and technology of domestic sewage for improvement of rural environment in China. *Journal of King Saud University–Science*, *34*(7), 102181.

Eryong, X., & Li, J. (2021). What is the ultimate education task in China? Exploring "strengthen moral education for cultivating people" ("Li De Shu Ren"). *Educational Philosophy and Theory*, *53*(2), 128–139.

Gao, S., He, L., Chen, Y., Li, D., & Lai, K. (2020). Public perception of artificial intelligence in medical care: Content analysis of social media. *Journal of Medical Internet Research*, *22*(7), e16649.

Garbuio, M., & Lin, N. (2019). Artificial intelligence as a growth engine for health care startups: Emerging business models. *California Management Review*, *61*(2), 59–83.

Garg, H. (2020). Digital twin technology: Revolutionary to improve personalized healthcare. *Science Progress and Research (SPR)*, *1*(1).

Guo, C., Zhang, J., Liu, Y., Xie, Y., Han, Z., & Yu, J. (2020). Recursion enhanced random forest with an improved linear model (RERF-ILM) for heart disease detection on the internet of medical things platform. *IEEE Access*, *8*, 59247–59256.

Iwendi, C., Khan, S., Anajemba, J. H., Bashir, A. K., & Noor, F. (2020). Realizing an efficient IoMT-assisted patient diet recommendation system through machine learning model. *IEEE Access*, *8*, 28462–28474.

Jiang, X., Xie, H., Tang, R., Du, Y., Li, T., Gao, J., Xu, X., Jiang, S., Zhao, T., Zhao, W., & Sun, X. (2021). Characteristics of online health care services from China's largest online medical platform: Cross-sectional survey study. *Journal of Medical Internet Research*, *23*(4), e25817.

Kadry, S., Rajinikanth, V., Rho, S., Raja, N. S. M., Rao, V. S., & Thanaraj, K. P. (2020). Development of a machine-learning system to classify lung CT scan images into normal/COVID-19 class. *arXiv preprint arXiv:2004.13122*.

Khan, S. A., Nazir, M., Khan, M. A., Saba, T., Javed, K., Rehman, A., Akram, T., & Awais, M. (2019). Lungs nodule detection framework from computed tomography images using support vector machine. *Microscopy Research and Technique, 82*(8), 1256–1266.

Manickavasagam, R., & Selvan, S. (2019). Automatic detection and classification of lung nodules in CT image using optimized neuro fuzzy classifier with cuckoo search algorithm. *Journal of Medical Systems*, *43*(3), 1–9.

Manimurugan, S., Almutairi, S., Aborokbah, M. M., Narmatha, C., Ganesan, S., Chilamkurti, N., Alzaheb, R. A., & Almoamari, H. (2022). Two-stage classification model for the prediction of heart disease using IoMT and artificial intelligence. *Sensors*, *22*(2), 476.

Mody, R. N., & Bhoosreddy, A. R. (1995). Multiple odontogenic keratocysts: A case report. *Annals of Dentistry*, *54*(1–2), 41–43.

Shahabaz, A., & Afzal, M. (2021). Implementation of high dose rate brachytherapy in cancer treatment. *Science Progress and Research (SPR)*, *1*(3), 77–106.

Sun, L., Jiang, X., Ren, H., & Guo, Y. (2020). Edge-cloud computing and artificial intelligence in internet of medical things: Architecture, technology and application. *IEEE Access*, *8*, 101079–101092.

Ter-Sarkisov, A. (2022). One shot model for COVID-19 classification and lesions segmentation in chest CT scans using LSTM with attention mechanism. *IEEE Intelligent Systems*.

Wang, X., Chen, H., Gan, C., Lin, H., Dou, Q., Tsougenis, E., Huang, Q., Cai, M., & Heng, P. A. (2019). Weakly supervised deep learning for whole slide lung cancer image analysis. *IEEE Transactions on Cybernetics*, *50*(9), 3950–3962.

Zhang, L., Lin, G., Gao, B., Qin, Z., Tai, Y., & Zhang, J. (2020). Neural model stealing attack to smart mobile device on intelligent medical platform. *Wireless Communications and Mobile Computing*, *2020*.